

## Calibration of the NuMI Beam Monitors

D.Indurthy<sup>1</sup>, S.Mendoza<sup>1</sup>, Z.Pavlovich<sup>1</sup>, R.Zwaska<sup>1</sup>, S.Kopp<sup>1</sup>, D.Harris<sup>2</sup>, A.R.Erwin<sup>3</sup>

<sup>1</sup>Department of Physics, University of Texas, Austin

<sup>2</sup>Fermi National Accelerator Laboratory

<sup>3</sup>Department of Physics, University of Wisconsin, Madison

### Abstract

We present an analysis of calibration studies of the NuMI Hadron and Muon Monitors. Each pixel response to gamma's from a 1 Ci <sup>241</sup>Am source is measured. A relative calibration accurate to 1% is achieved for the muon beam monitors, and a 2% relative calibration is achieved for the hadron beam monitor. In addition, coefficients are measured to characterize temperature- and pressure-induced variations of the ion chambers' response.

## 1 Introduction

The NuMI secondary and tertiary are monitored by the hadron monitor [1] and muon monitors [2] respectively. Their purpose is to align the remnant hadron beam at the end of the decay pipe providing transverse spatial profiles of the hadron and muon beam downstream of the absorber, as well as providing relative measurements of secondary and tertiary beam intensities. The hadron monitor and muon monitors are arrays of ion chambers in He-filled vessels.

A 5% relative calibration of the chambers within the Hadron Monitor is required. The hadron monitor is designed as a  $7 \times 7$  array of ion chambers evenly spaced over a  $1\text{m} \times 1\text{m}$  transverse area[1]. The chambers are oriented such that the electrodes are normal to the beam. A 5% relative calibration of each chamber provides a beam centroid determination within 3cm, which corresponds to a  $42 \mu\text{rad}$  alignment of the beam [3].

The Muon Monitor requires a 1% relative calibration of its ion chambers. The muon monitors consist of  $9 \times 9$  arrays of 3mm-spaced ion chambers in 3 alcoves. Dolomite rock interspersed between the alcoves filters out lower momentum muons. Therefore, successive muon monitors detect decay products of higher energy parents. A 1% chamber-to-chamber calibration to of all three alcoves' chambers is required to achieve a beam alignment of  $100 \mu\text{rads}$  and to permit use of the relative pulse heights in each alcove as a coarse check of the beam's energy spectrum[4].

This paper will describe the procedure used to calibrate these detectors, the relative scale factors derived, and checks performed to verify the integrity of the process. The central results are the relative scale factors in Tables 4 through 7.

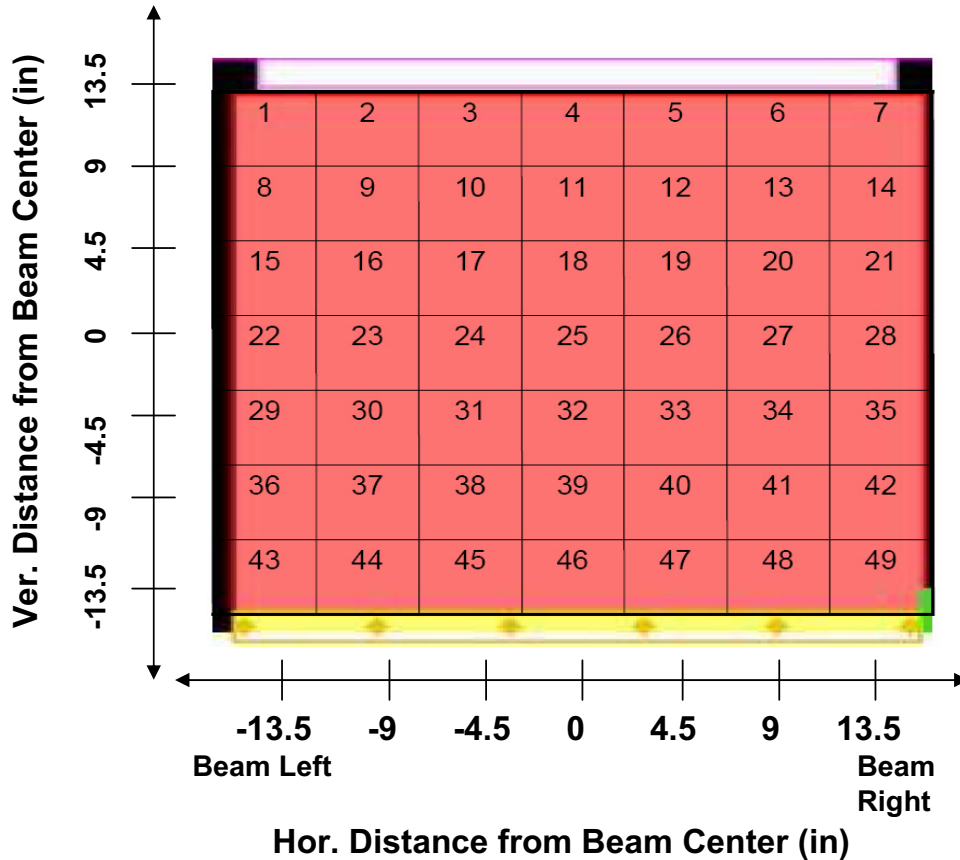


Figure 1: Beam’s eye view of the hadron monitor. The chambers are numbered according to the scheme used for the calibration process.

## 2 Chamber Mapping Conventions

Figure 1 shows the numbering scheme for indexing chambers in the hadron monitor during calibration. Chambers increment from left to right. This chamber ordering is identical to the channel mapping in the readout electronics in the NuMI beam.

The channel convention for muon monitors was not the same during the calibration procedure as it was as installed in the NuMI beam. The NuMI convention for the readout electronics is shown in Figure 2: channel 41 within a muon alcove array is at beam center, while channel 1 is to the beam left and in the upper-most corner. During the construction and calibration procedure, we numbered tubes consecutively from 1 to 32, in chronological order of fabrication and within a tube, the chambers were numbered from 1 to 9 starting from the feedthrough end of the muon tube, as shown in Figure 3. We adopt the scheme that “Chamber number” runs from 1 through 9 starting at the feedthrough end of the tube, while “Channel number” runs from 1 through 81 and refers to the as-installed positions of the pixels in the NuMI beam, as given in Figure 2.

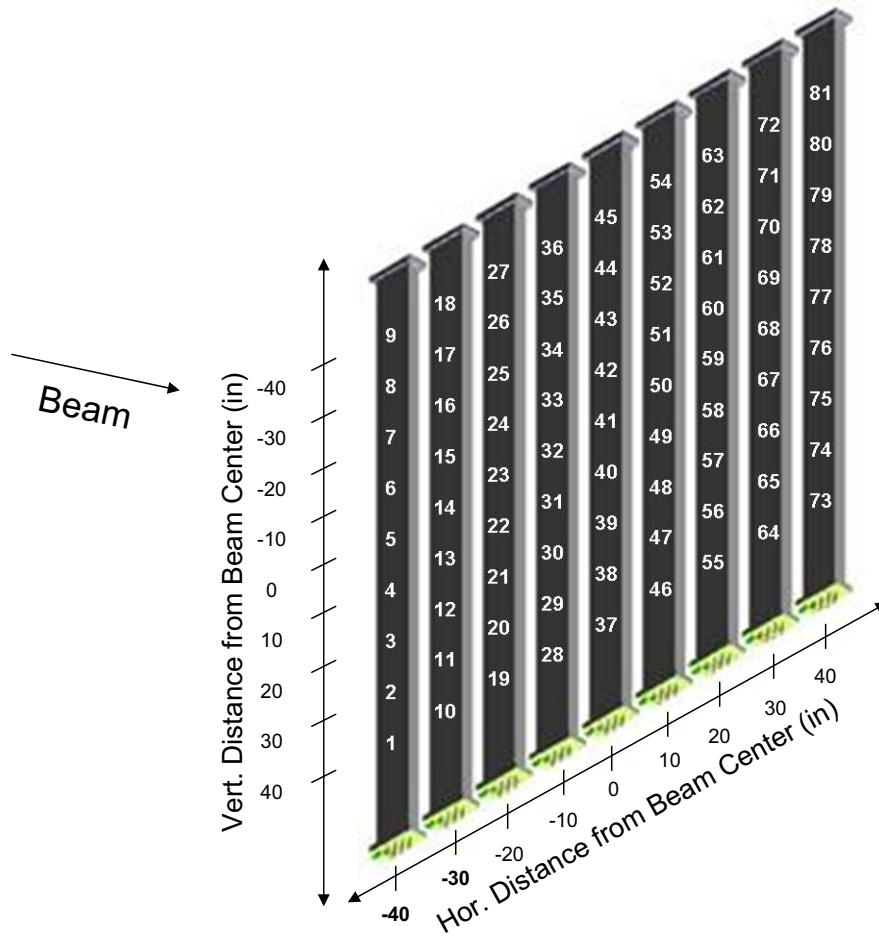


Figure 2: An isometric beam's eye view of the muon monitor array as installed in the NuMI beam. The chambers are numbered according to the channel number used by the readout electronics, incrementing upward and toward beam right.

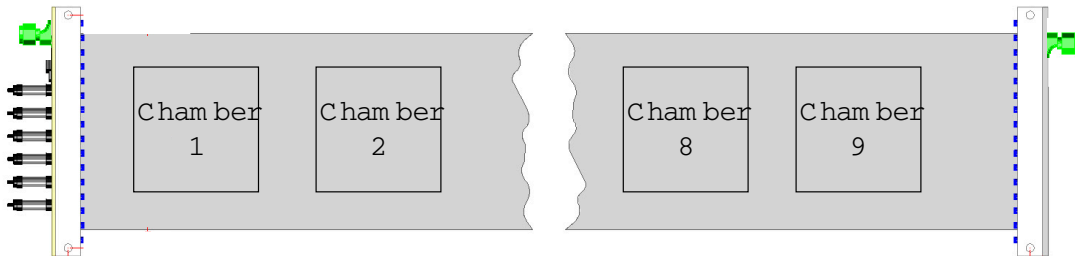


Figure 3: A single muon tube with indices corresponding to the calibration mapping of chambers.

### 3 Calibration

The relative calibration of each chamber in the muon and hadron monitors was achieved by mapping each chamber with a 1 Ci  $\text{Am}^{241}$  gamma source. The induced ionization current was compared from chamber to chamber after systematic effects such as source alignment with respect to each pixel or temporal variations such as gas pressure and temperature were factored out.

The hadron monitor could be tested within 8 hours, over which time systematic drifts or pressure changes in the gas were not significant. The 32 muon monitor tubes, having been constructed over the period of approximately one year from September, 2003, to August, 2004, posed more significant challenges to calibrate: the 9 chambers within a tube could be calibrated within less than 8 hours, but the time between calibrations of consecutive tubes could be up to weeks.

The calibration apparatus had to control for systematic variations over such long periods. First, the gas system purged the chambers with pure gas and had instrumentation for measuring pressure, temperature, and impurity levels. Second, a control ion chamber, with its own internal calibration source, was mounted in series with the chambers being calibrated in the gas system; any temporal variations in the gas system would thus be observed in the control, or reference, chamber. Third, the electronics were re-calibrated for drift with each chamber to be calibrated.

#### 3.1 Source

A 1 Ci  $^{241}\text{Am}$  gamma source is used to irradiate each ion chamber in both the hadron monitor and muon monitors[5].  $^{241}\text{Am}$  has a half-life of 433 years. The source is housed in a steel capsule within a cylindrical lead pig for shielding.  $^{241}\text{Am}$  emits an  $\alpha$  particle to form an excited state of  $^{237}\text{Np}$  which in turn emits a 60 keV  $\gamma$  as it deexcites. The  $\alpha$  particles are captured in the steel capsule, and the gammas proceed through an aperture in the lead pig.

Beam scans were performed across a single muon monitor chamber to understand beam collimation of the source. As shown in Figure 4, a 1" diameter opening on the lead pig produces an uncollimated beam with a FWHM of about 8cm. Such a wide field of illumination is desirable, because in this case the source illuminates the entire  $8 \times 8 \text{ cm}^2$  sense pad of the ion chambers. The unfortunate trade-off is that the increased sensitivity of our calibration results to accurate placement of the source near the ion chamber. A second scan was performed with a 1/4" collimator made of brass. In addition to producing less detectable signal in the muon monitor, the flat chamber response from 7 to 11cm for the collimated beam suggests that tightly-collimated source does not illuminate the entire sensitive area of the chamber. Since the chamber sense-pad is 7.6cm wide, the inferred width of the collimated beam is 1.8cm. Furthermore, the long tail of signal observed in the ion chamber even when the collimated source is placed 17 cm off-center suggests there is scattering of the low-energy gammas in the collimator brass at a level of 50% of the detectable signal. With these trade-offs in mind, we opted for use of the wider 1" collimator opening, having to establish more

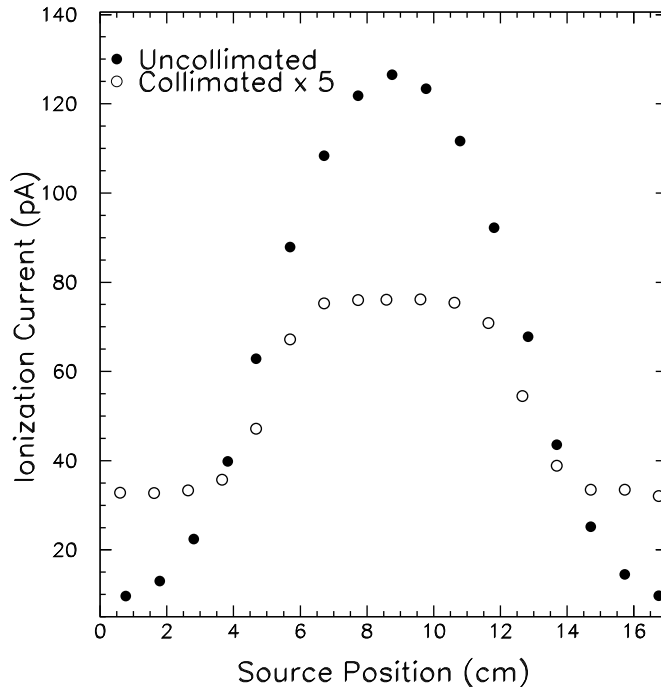


Figure 4: Beam scans with beam collimated to 1" and 1/4".

stringent alignment of the source relative to the ion chambers for each of the calibrations.

Figure 5 shows the result of a fine-stepped scan of the 1 Ci source across a couple of the chambers in the Hadron Monitor. It is clear that the source illumination is never entirely contained within the ion chamber, since the ionization current never comes to a flat plateau. However, it may be seen that the current does not deviate by greater than one percent unless the source is misplaced from the chamber center by greater than 0.2 inches. The desire to calibrate our Hadron Monitor chambers to better than 1% over all thus suggested a design of a stand which aligns the source pig in front of each chamber to better than 1/8".

Figure 6 shows the result of a fine-stepped scan of the 1 Ci source across a couple of the chambers in the Muon Monitor tube 29. In the left graph, chamber 6 is scanned in the horizontal direction and the reference chamber is simultaneously read out to monitor stability. In the right graph, both chambers 1 and 9 are scanned vertically so as to check that the muon tube is level. A similar behaviour is observed as with the Hadron Monitor, namely that the source illumination is never completely contained in the ion chambers. However, it is similarly true that placing the source within 1/16" accuracy around the ion chamber center is sufficient to cause no worse than a 0.5% systematic uncertainty in the induced ionization current.

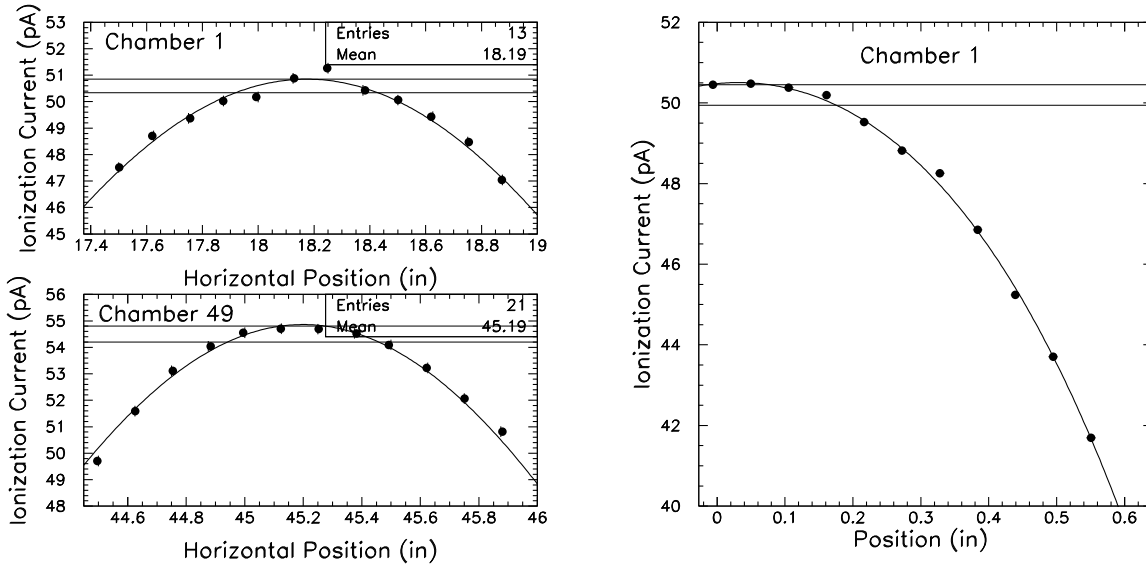


Figure 5: A fine scan of chamber 1 in the hadron monitor in the horizontal (left) and vertical (right) directions. The point at 0" is the aligned operating position. The curves indicate that placement of the source to within  $\pm 0.2''$  is sufficient to maintain a 1% repeatability in calibration.

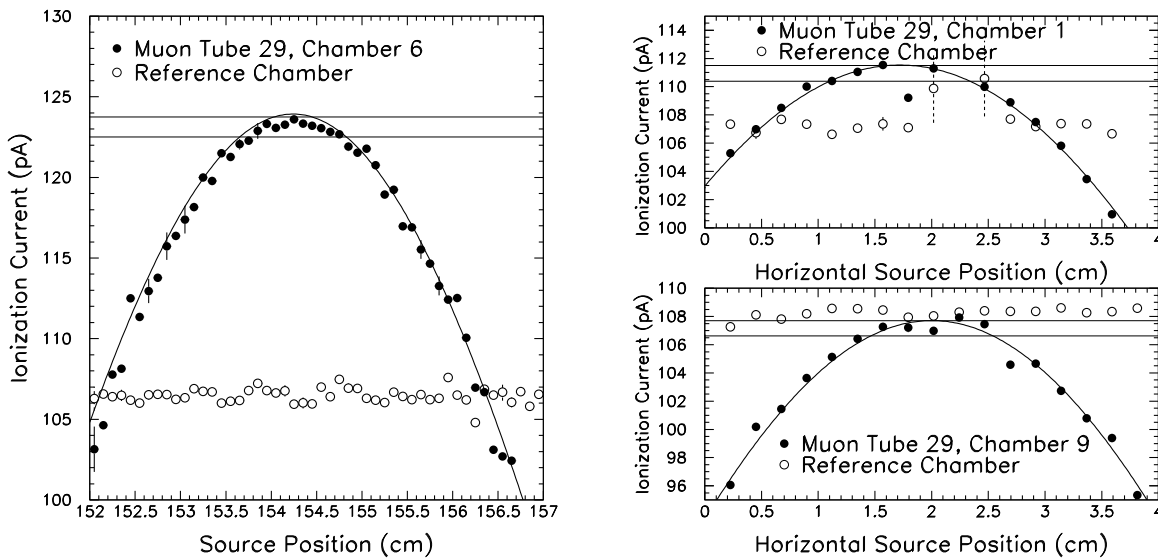


Figure 6: (left) Fine scan in the horizontal direction of chamber 6 of muon tube 29. (right) Fine scan in the vertical direction of chambers 1 and 9 of muon tube 29.

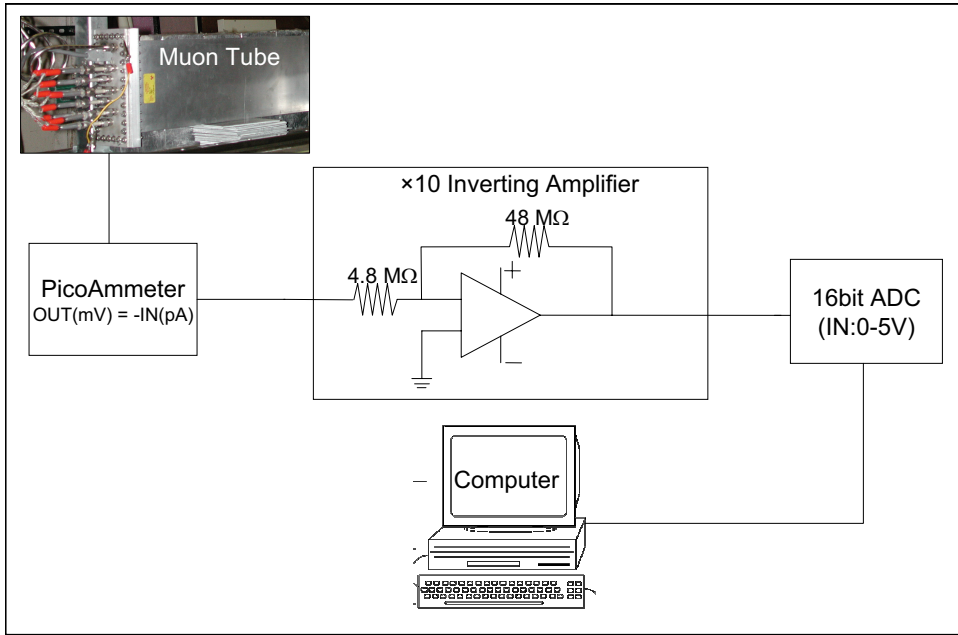


Figure 7: Schematic of the ionization chamber readout.

### 3.2 Electronics

Figure 7 shows a schematic of the readout of the chambers for the Muon and Hadron Monitor calibrations. The components of the electronics include:

- A Keithley 230 GPIB-controllable DC power supply provides a bias voltage to the ion chamber which is programmed to scan between -100 V and 100 V in 10 V increments with 10 mV precision[6].
- Eight Keithley model 480 and 485 picoammeters [6] were used to read out the ionization current from the chambers being tested during the calibration scans. The picoammeters have resolution of order 0.1 pA, as is discussed below. Most produce an analog output voltage proportional to the measured ionization current, while two are GPIB-controllable and can be read back to the computer directly.
- A 16-bit Analog-to-Digital Converter converter 0-5 Volt input, Model TNG-1 by Mindtel, Inc.[7] which reads the analog outputs of the picoammeters. The least count of the ADC corresponds to approximately 0.08pA. The ADC is read into the computer over the serial bus.
- A custom NIM module with 8 channels of op amp circuits to invert the picoammeter outputs and scale them to 0-5 V before they are fed in to the ADC.

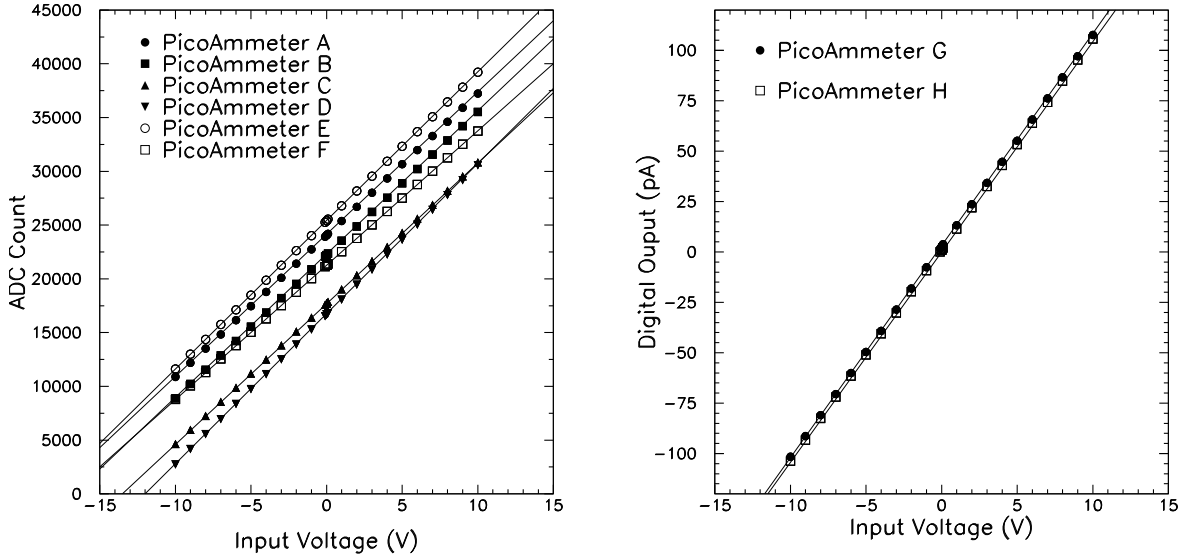


Figure 8: Calibration of the Keithley picoammeters. Six picoammeters were readout from their analog outputs through an ADC(left). Two picoammeters had digital outputs that were recorded directly (right).

The eight picoammeters were individually calibrated by applying -10 to 10 mV across a resistor measured to be  $100.04 \text{ M}\Omega$ . The voltage was supplied from the Keithley 230 supply, which has  $10 \text{ }\mu\text{V}$  precision when used in its  $\pm 100 \text{ mV}$  range. The results of the calibrations are shown in Figure 8. All picoammeters are shown to be linear with input current with residuals on the order of  $0.1 \text{ pA}$ . There is more variability in the slope of the picoammeters read out by the ADC due to variations in the resistors and operational amplifiers used in the NIM module for amplification of the picoammeter analog outputs.

Nominally, the picoammeters' digital display is significant to  $1 \text{ pA}$ , but we found that the analog voltage output provides measurement precision to  $0.1 \text{ pA}$ . The reason for the  $1 \text{ pA}$  display appears to be that the picoammeters experience drift of up to  $0.07 \text{ pA/hr}$ . This drift is empirically found to be acceptably small over the  $\sim 30$  minutes of an ion chamber calibration in order to exploit the potential  $0.1 \text{ pA}$  resolution of the picoammeters: as shown in Figure 9, a voltage bias curve taken of either a hadron or muon monitor chamber shows the characteristic rise to ionization current plateau by  $\sim 10 \text{ V}$ , and the plateau is steady to far better than  $1 \text{ pA}$ . Such voltage bias curves require approximately 30 minutes to acquire, which sets the scale for the duration over which the picoammeters are stable. As can be seen in Figure 10, however, over periods of several hours the picoammeter output does experience drift of order  $2 \text{ pA}$ : in this figure, bias voltage scans are made for a single muon ion chamber which is illuminated by only its  $1 \text{ }\mu\text{Ci}$   $\alpha$  source. The ionization current on plateau should be constant, but varies by a couple picoamps over the 40 hour period.

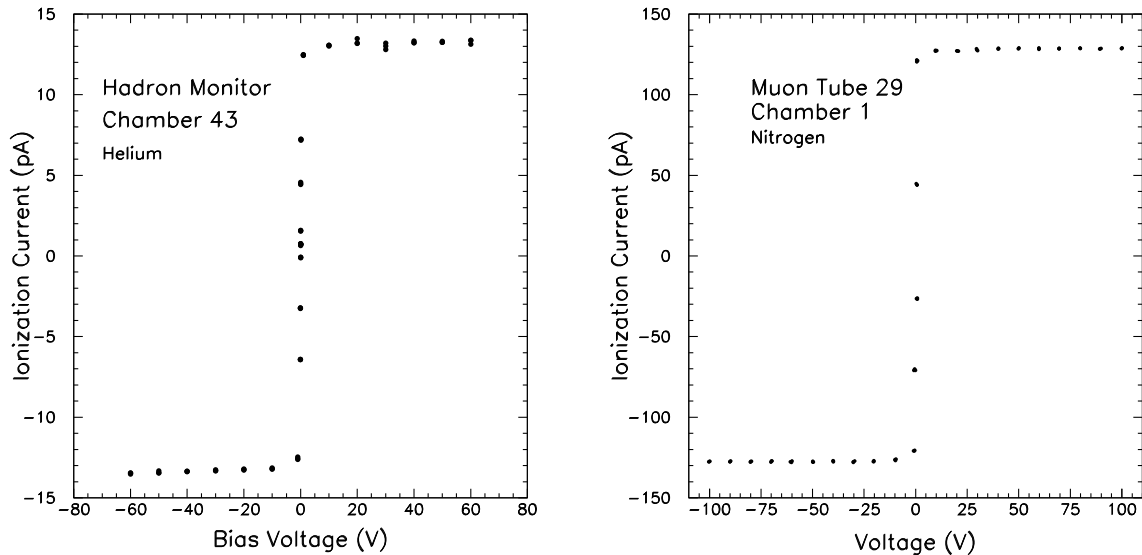


Figure 9: Voltage bias curves for a single ion chamber in the Hadron Monitor (left) and a Muon Monitor tube (right).

To combat the effect of the picoammeter drift, we ramped the ion chamber bias voltages from  $-100$  to  $+100$  Volts for every ion chamber that we measured. In this way, a plateau value for the ionization current is measured for both the positive and negative voltage polarity. In principle, these values should be the same, and the extent to which they differ in absolute value is a measure of the drift in the picoammeter circuit. We define

$$I_{\text{plateau}} = \frac{1}{2}(I_+ - I_-)$$

$$I_{\text{offset}} = \frac{1}{2}(I_+ + I_-)$$

where  $I_+$  is the average of the ionization currents measured for all bias voltages above  $20$  V and  $I_-$  is the average of the ionization currents measured for all bias voltages below  $-20$  V (which as shown in Figure 9 has the opposite sign as  $I_+$  due to the collection of electrons at the signal plate as opposed to the collection of ions in the case of  $I_+$ ). The quantity  $I_{\text{plateau}}$  is a measure of the plateau ionization current that is less sensitive to picoammeter drift than just taking  $I_+$  alone, while the quantity  $I_{\text{offset}}$  is a useful measure of the picoammeters' drift. Figure 11 shows the quantities  $I_{\text{plateau}}$  and  $I_{\text{offset}}$  as a function of time during the 40 hours of repeated voltage bias curves from Figure 10

During the same 40 hour period, the offset and plateau ionization current were read out for a muon monitor chamber exposed to the  $1$  Ci source. This data is shown in Figure 12. Like the chamber reading out only the  $1$   $\mu\text{Ci}$  source, the offset drifts by about  $2$  pA and the plateau ionization current  $I_{\text{plateau}}$  is constant to better than  $0.5$  pA.

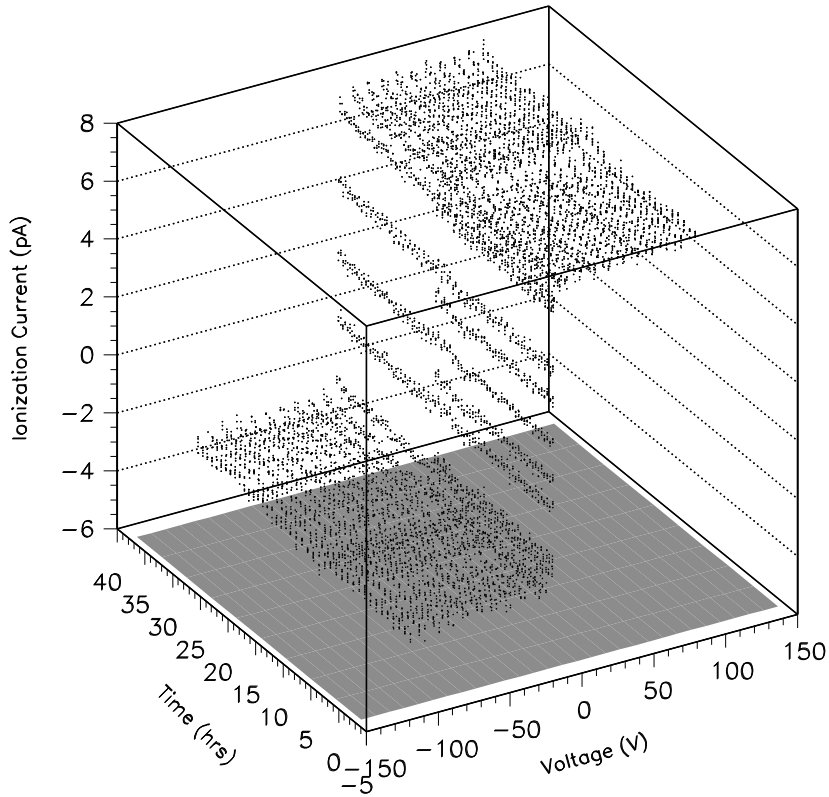


Figure 10: Repeated bias voltage curves obtained over a 40 hour period. The ionization current is read at several voltages from -100 V to 100 V, and the voltage sweep is subsequently repeated.

In Figure 13 we show a separate study of the repeatability of the ionization current measurement which tests both the stability of the electronics and also the repeatability of the placement of the 1 Ci source in front of a chamber. In this study, the 1 Ci source is moved back and forth between chambers 6 and 7 within a single muon tube. At each placement of the 1 Ci source, the plateau ion current  $I_{\text{plateau}}$  is read out of both chambers. The irradiated chamber reads approximately 124 pA, while the non-irradiated chamber sees the few picoamps from its internal calibration source. For both chambers, the repeatability of these measurements is approximately 0.25pA, irrespective of whether the signal is 5 pA or 124 pA.

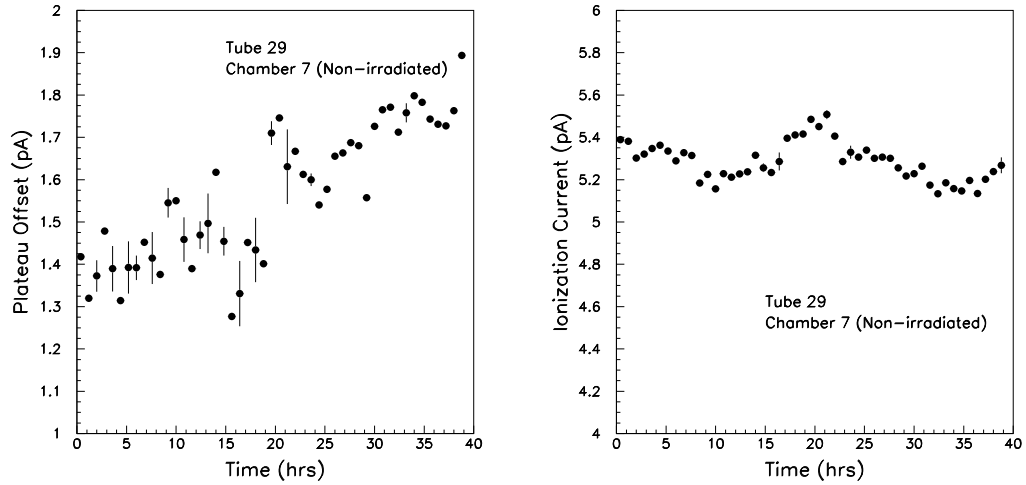


Figure 11: (left) Plateau curve DC offset  $I_{\text{offset}}$  over the duration of the repeatability study. (right) Derived plateau ionization current  $I_{\text{plateau}}$  over the duration of the repeatability study.

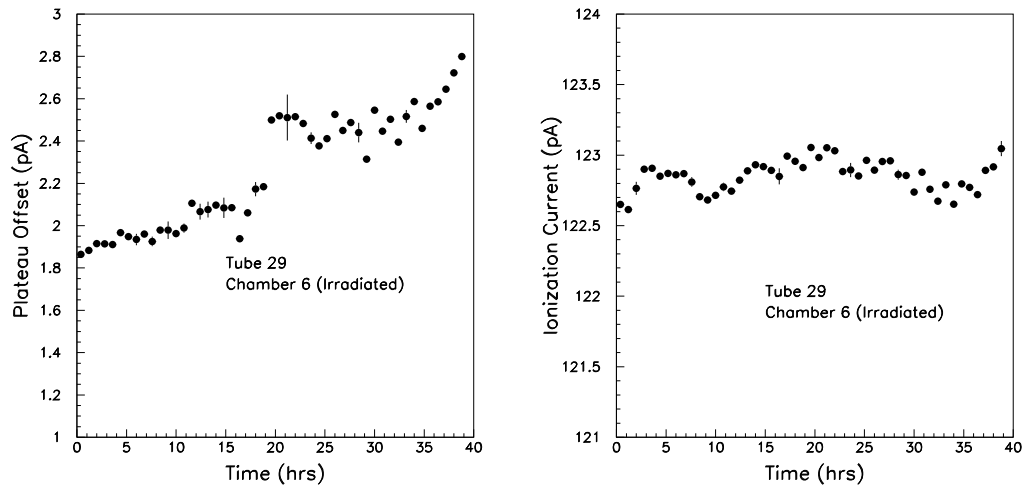


Figure 12: Offset and plateau ionization current for chamber 6 of a muon tube which is exposed to the 1 Ci source. The data come from the the same 40 hour period as the data for the un-irradiated chamber from Figure 11.

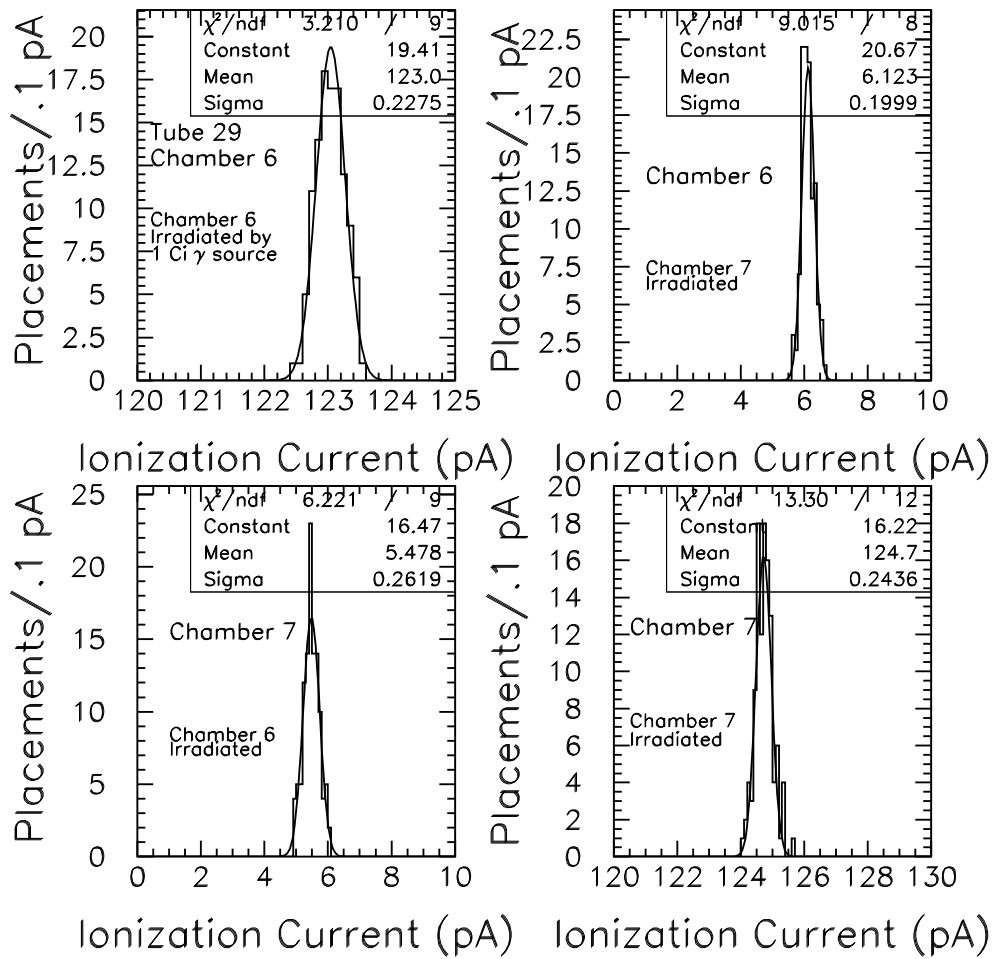


Figure 13: Histograms of the repeated plateau height measurements from chambers six and seven as the source placement is alternated.

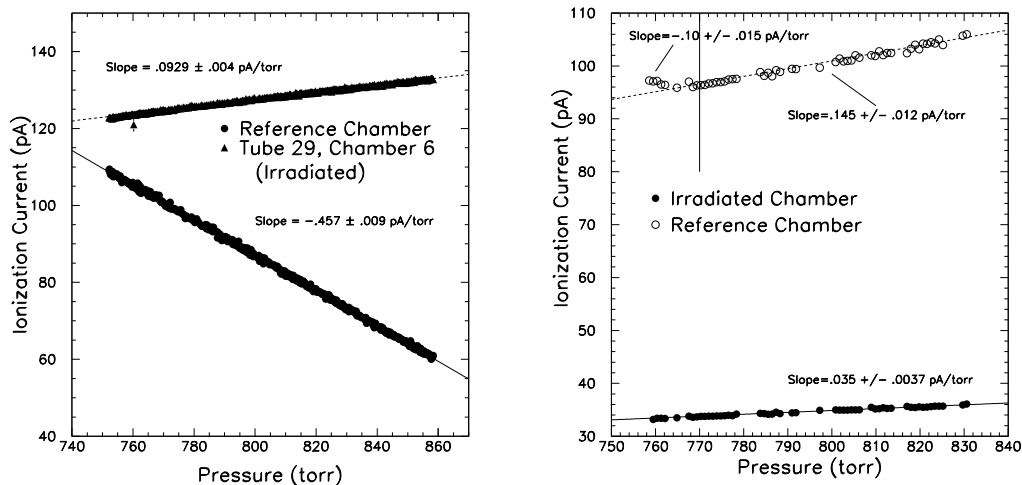


Figure 14: Change in response of the ionization current in variation with pressure in N<sub>2</sub> (left) and He (right) gas.

### 3.3 Gas System

Ambient temperature is constantly recorded by the Applied Data Sciences Weather Logger which is sensitive to 1° F changes[8]. Pressures are monitored by an MKS 750B pressure transducer installed directly upstream of the detector[9]. It is sensitive to 0.1 torr variations.

A reference chamber is installed downstream of the Hadron/Muon Monitor in the same gasline as the detector. It serves as an additional monitor of temperature and pressure variations. It is a single, 3mm gap chamber in an stainless steel vessel. It's gas volume is illuminated by 40 1μCi of α sources to provide a standard signal. These sources are specifically lining the walls of the vessel, so there is about a .5" distance between the sources and the chamber gap. The reference chamber is shown to be sensitive to fluctuations in pressures, temperatures, and provides a measure of the accuracy of our corrections.

The muon monitors were calibrated over a period of ~1 year, during which time pressures varied by as much as 10 Torr, and temperatures by 20 degrees. Since the measured ion current of a given chamber varies with these quantities, it is desirable to correct for such variations via

$$I_{\text{plateau}}^{\text{CORR}} = I_{\text{plateau}}^{\text{raw}} \times [1 + A(T - T_{\text{nominal}})] \times [1 + B(P - P_{\text{nominal}})]$$

where  $I_{\text{plateau}}^{\text{raw}}$  ( $I_{\text{plateau}}^{\text{CORR}}$ ) refer to the raw (corrected) plateau ionization currents,  $P$  and  $T$  refer to absolute pressure in Torr and to temperature in °F, and  $T_{\text{nominal}} = 75^{\circ}\text{F}$  and  $P_{\text{nominal}} = 790$  Torr refer to nominal pressure and temperature conditions.

We derive the constants  $A$  and  $B$  above from Figure 14 and Figure 15. These show the ionization current of an individual muon chamber and the reference chamber as a function of pressure or temperature in N<sub>2</sub> and He gases. Pressure was varied via adjusting a metering

Pressure Scans	He		N <sub>2</sub>	
	Nominal Signal (pA)	Slope (%/torr)	Nominal Signal (pA)	Slope (%/torr)
Irradiated	34.5	0.10	125	0.09
Non-Irradiated	2-3	0.17	4-8	-0.055
Reference	95	0.15	101	-0.46
Temperature Scans	He		N <sub>2</sub>	
	Nominal Signal (pA)	Slope (%/torr)	Nominal Signal (pA)	Slope (%/torr)
Irradiated	27.4	0.35	124.5	-0.076
Non-Irradiated	3-5	1.3	6-8	-.27
Reference	85.8	-0.230	108	0.67

Table 1: Variations of plateau height with pressure and temperature in He and N<sub>2</sub> gas. The slopes are fits to the graphs in Figures 14 and 15. The correction constants  $A$  and  $B$  (see text) are  $(-1)$  times these slopes.

valve downstream of the reference chamber while maintaining constant flow. Ionization currents were read out from the reference chamber and the chamber irradiated by the 1 Ci source. In nitrogen, the ion chambers and reference chamber show opposite trends. As the density of the gas increases with pressure, there are two competing effects at work: there is greater ionization in the chamber gap, but there is also a greater probability of radiation interacting before it enters the gap. For the irradiated chamber, the former effect dominates. For the reference chamber, more alpha's range out with increased nitrogen density before reaching the chamber volume, producing less ionization in the chamber gap. In Helium, the reference chamber shows both these effects as the pressure is increased beyond 770 Torr.

The results of several temperature scans are illustrated in Figure 15. During these scans, the ambient temperature was varied by 6-10 °F adiabatically over a period of 24 hours. The reference chamber again shows an opposite trend to that of the irradiated chamber, as lower temperature gas causes alpha's to range out before entering the chamber gap.

The derived pressure and temperature constants  $A$  and  $B$  are summarized in Table 1.

As a test of these temperature and pressure corrections, we studied the ionization current from the reference over the course of the 400 days of calibrations. Figures 16 and 17 show the ionization current measurements of the reference chamber obtained during the 400 days muon chamber calibrations. Shown are the temperature and pressure during thistime, as well as the signal from the reference chamber, before and after corrections. As shown in Figure 17, the calibrations leave a spread of only 0.6 pA out of a signal of 100 pA. Thus the reference chamber can be calibrated to better than 1%. Furthermore, because the reference chamber is five times more sensitive to pressure and temperature variations than the actual Muon and Hadron Monitor ion chambers, we conclude that the gas monitoring system satisfactorily controls for such variations.

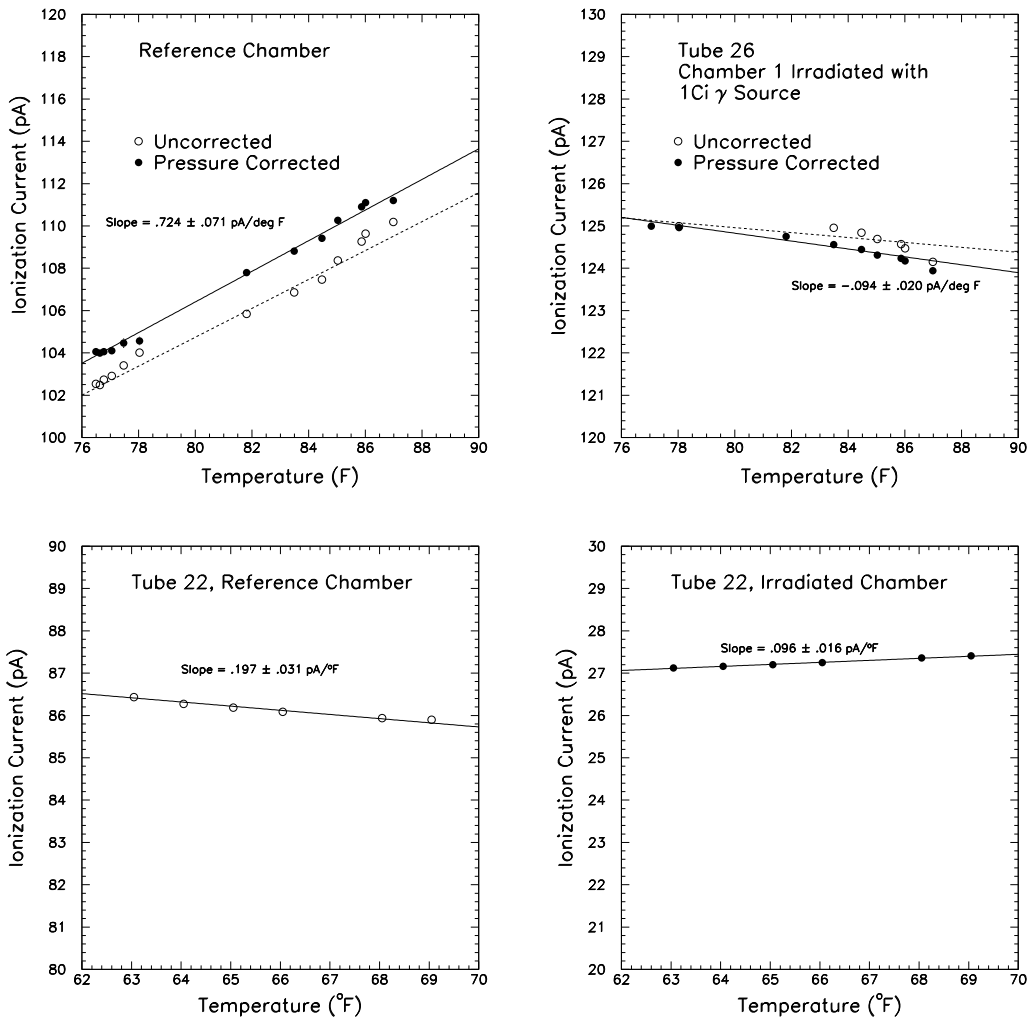


Figure 15: Temperature scans of muon chambers in N<sub>2</sub> (top row) and He (bottom row) gas. Shown are the ionization currents in the reference chamber (left column) and a muon tube ion chamber illuminated by the 1 Ci source (right column).

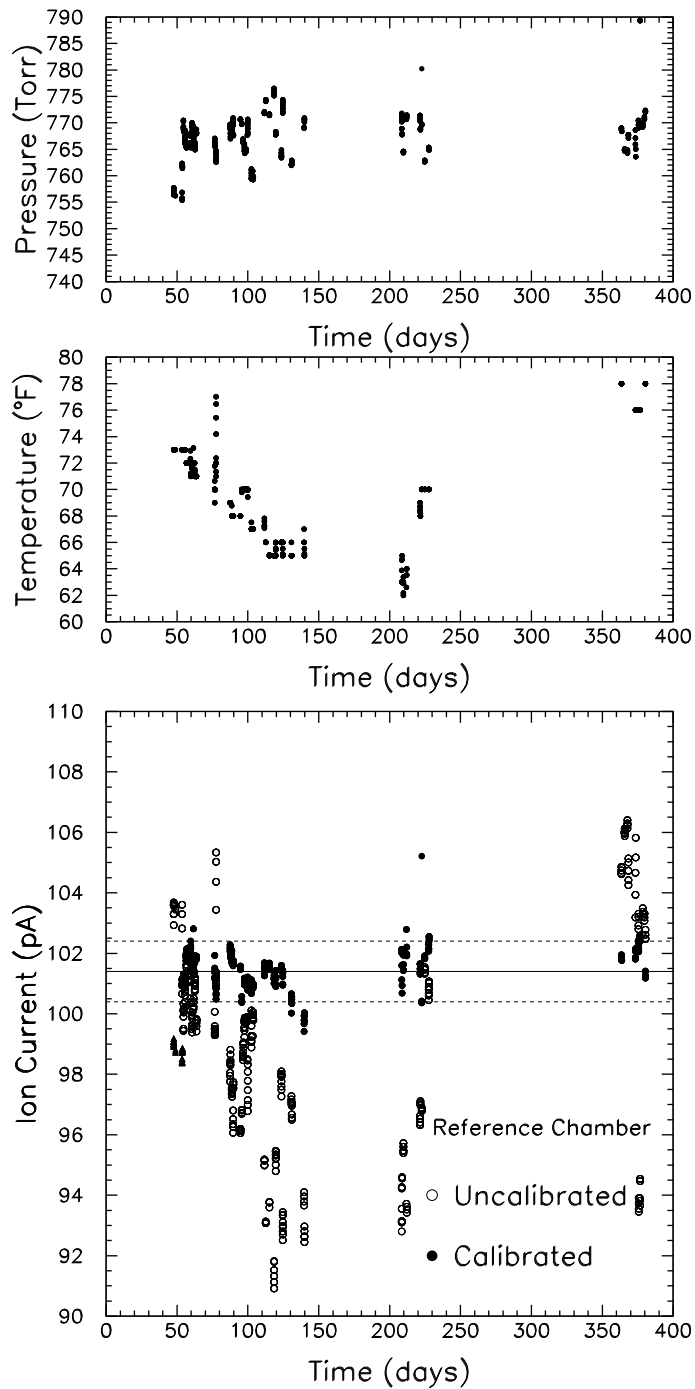


Figure 16: Graph of absolute pressure (top) and of temperature (middle) for the reference chamber over the 400 days of calibration operations. (bottom) The ionization current in the reference chamber without and with the corrections for pressure and temperature variations.

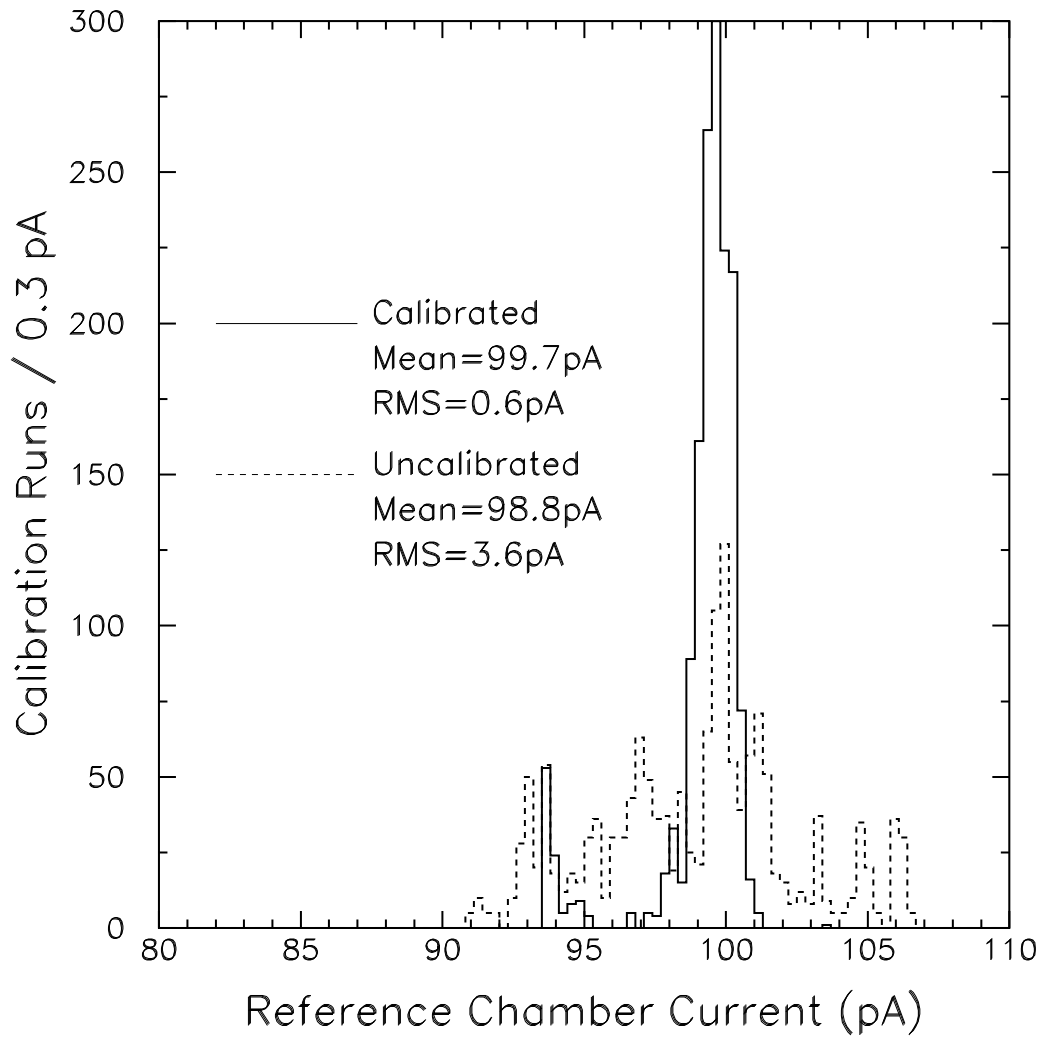


Figure 17: Histogram of reference chamber currents for every muon chamber calibration. The raw and calibrated distributions are shown.



Figure 18: Hadron Monitor test stand.

## 4 Calibration Test Stands

### 4.1 Hadron Monitor

Figure 18 shows the test stand with the hadron monitor sitting on a horizontal beam mounted to vertical I-beams. Leveling mounts allow for precise alignment of the horizontal beam. The vertical beams are bolted to a wall and aligned with bubble levelers. The radiation source is supported by a second horizontal I-beam mounted on the vertical bars. The source support rail can be positioned to align the source with each row of pixels in the Hadron Monitor. A moveable cart allows for an arbitrary lateral positioning of the source. A tape measure is inlaid between the rails and bolted to the source bar to provide a means for consistent source placement.

Transverse scans of the detector were performed to confirm alignment of the test stand and to map out chamber centers. The source was placed at the far end of the source bar, and signals were recorded from all 7 chambers as the source was moved in  $1/2''$  increments across the detector. Figure 19 shows a coarse transverse scan across row 1. The fits indicate the chamber centers are evenly spaced by  $4.5''$  as designed. It also indicates the beam half-width from the radiation source is about  $1.5''$ . Since the sense pad of a chamber plate is  $3'' \times 3''$ , we illuminate the entire sensitive region of the chamber gap. Figure 5 shows a finer horizontal scan of chamber 1 and chamber 49 in  $1/8''$  increments.

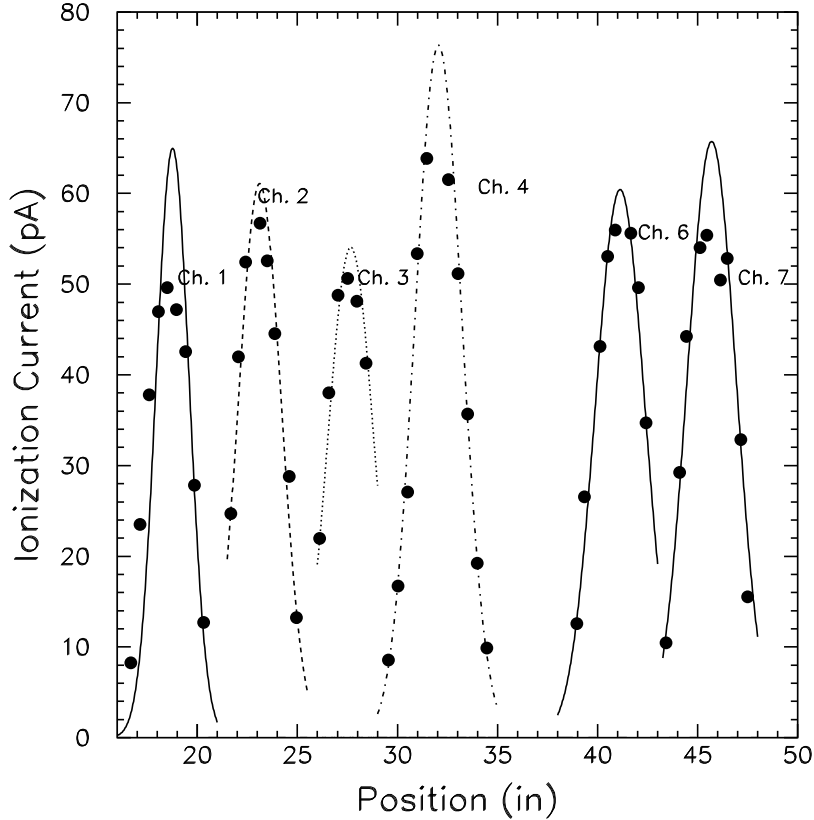


Figure 19: A coarse transverse scan of one row of the hadron monitor(chamber 5 not shown).

## 4.2 Muon Monitor

Figure 20 shows the test stand constructed to perform the muon tube calibrations. The tube is fixed to two vertical struts bolted to the surface of a lab table. A rail is also bolted to the table in front of the tube to guide a movable cart that supports the radiation source. The cart is machined to provide accurate vertical positioning of the pig. Signal output and HV lines are accessible at the endplate.

As in the case of the hadron monitor, scans were conducted to confirm alignment and map out chamber centers. Figure 21 shows a coarse transverse scan of a muon tube. The centroids are shown to be spaced by 10" as expected by design. A finer scan of chamber 6 was shown in Figure 6.

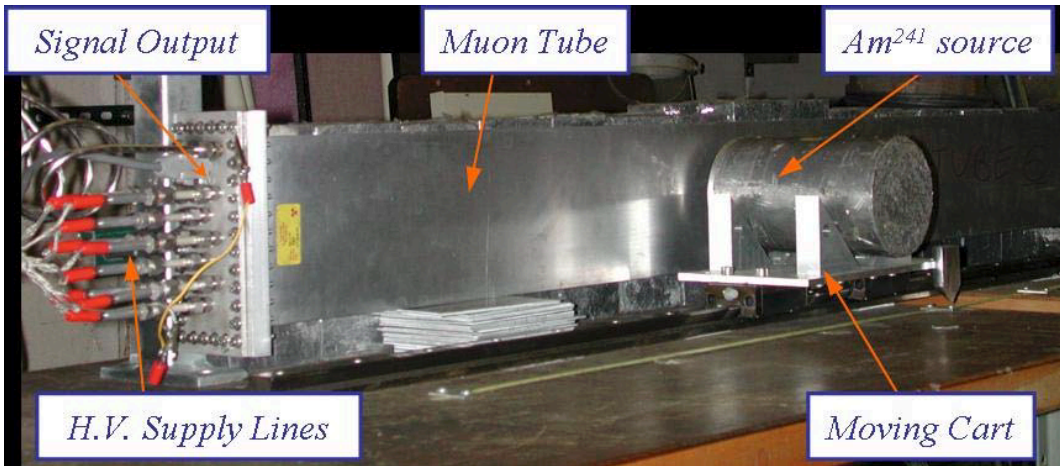


Figure 20: Muon monitor test stand.

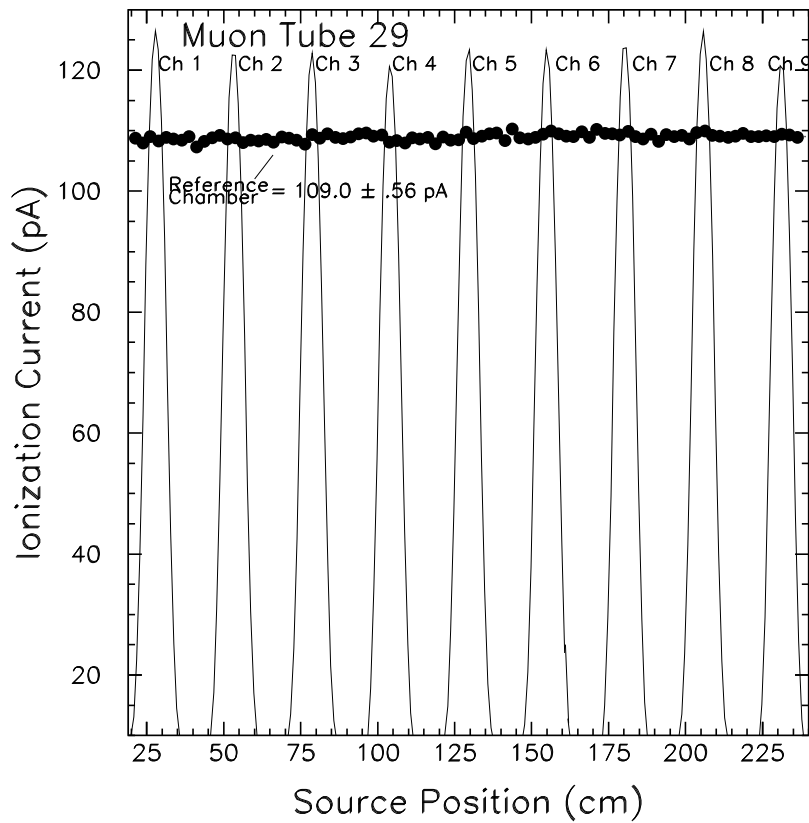


Figure 21: Coarse transverse scan of the muon monitor.

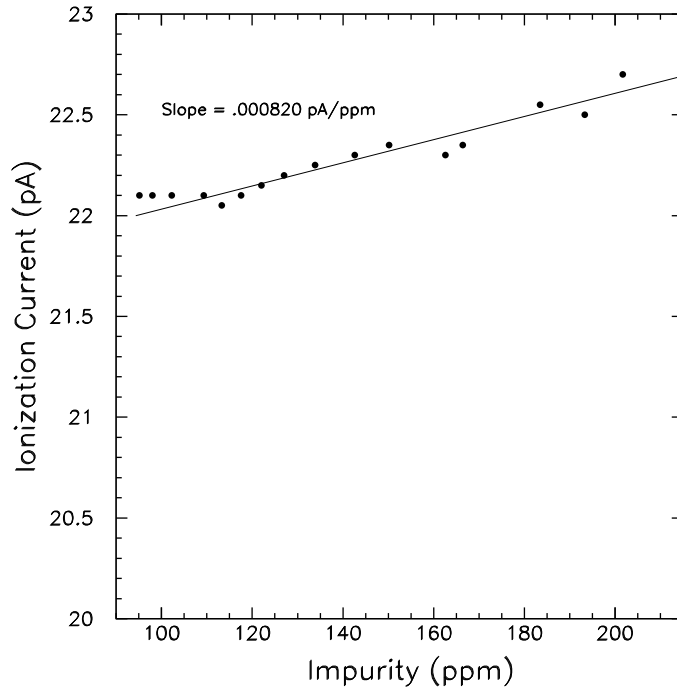


Figure 22: Ionization current in the Hadron Monitor as a function of O<sub>2</sub> impurity.

## 5 Calibration Analysis

### 5.1 Hadron Monitor

The hadron was calibrated over a period of 7 days. Each chamber response to the 1 Ci <sup>241</sup>Am gamma source was measured according to the procedure described above, and the calibration was repeated several times to check for consistency. Since the Hadron Monitor is a small, single vessel, each calibration run required approximately 5 hours.

A series of three full scans were performed in which all 49 chambers were tested. Additionally, two partial scans were performed to repeat measurements on one or two rows only. Table 4 summarizes the results of these calibration scans. Each column of the table represents one calibration run. Each of the 49 rows of the table is the data from one of the chambers. One full calibration run was performed in air, one in pure Helium, and one was taken while the chamber was being purged.

The ionization currents from every chamber have been divided by the current from chamber 25 (the middle pixel) within a given run. This scaling corrects for pressure or temperature changes that occurred in between calibration runs (again, assuming that the pressure change within a calibration run was small).

In the scan labeled HeCal2, it was noticed after the fact that the purity level dropped

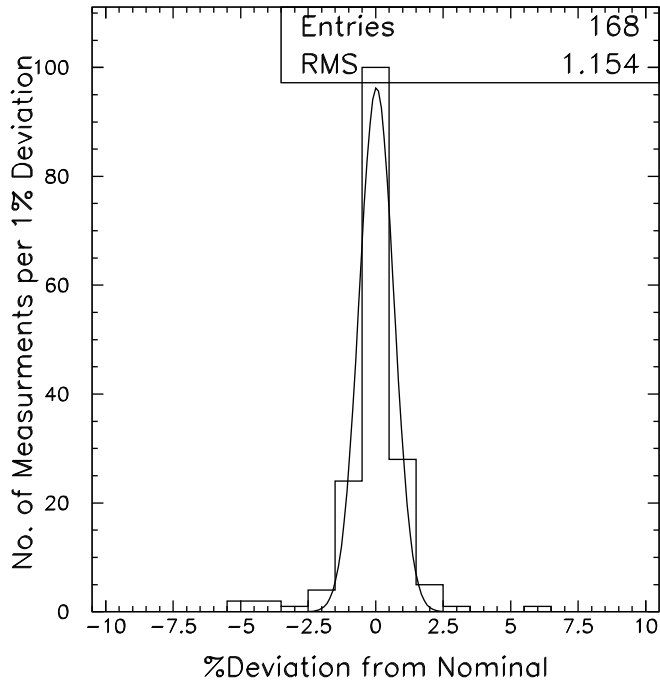


Figure 23: Histogram of the deviations of every ion chamber plateau height measurement during the Hadron Monitor calibration from the 'nominal' measurement, where 'nominal' refers to the values of HeCal4 in Figure 4.

over 45 ppm during the test due to initial purging of the Hadron Monitor with He gas. This dropping impurity level changed the chambers' response. In a separate test, the ionization current of chamber 49 was measured as a function of varying purity. The result is shown in Figure 22. A variation of 45 ppm is shown to correspond to an ionization current correction of up to .25 pA. We therefore use the trend of Figure 22 to correct the calibration run HeCal2. Table 4 shows both the uncorrected and corrected measurements for the HeCal2 scan.

The values within a given row of Table 4 should be identical if the calibration runs were perfect. Fluctuations within a row result from measurement uncertainties in the calibration (source placement, pressure variation, electronics noise). We plot the deviations of the normalized plateau height from nominal are shown in Figure 23. 'Nominal' refers to the chamber values obtained from the scan labeled HeCal4. The halfwidth of Figure 23 is 1.2%, with only 2 outliers ranging beyond  $\pm 5\%$ . The outliers are measurements from two different chambers and can be attributed to incorrect source placement for those particular plateau height measurements. Thus, we conclude that the individual chamber response of every pixel in the hadron monitor is understood relatively to better than 2%.

Table of Errors	Muon Chamber		Ref. Chamb.	
	N <sub>2</sub>	He	N <sub>2</sub>	He
Electronics	0.1%	0.1%	0.2%	0.2%
Source Placement	0.8%	0.8%	–	–
Pressure Correction	0.05%	0.1%	0.1%	0.15%
Temperature Correction	0.1%	0.3%	0.3%	0.2%
Total Uncertainty	0.9%	1.0%	0.5%	0.5%

Table 2: The contributions to the uncertainty of the plateau measurement for the Muon Monitor chambers being calibrated and for the Reference Chamber being measured in parallel.

## 5.2 Muon Monitor

The muon monitor ion chambers were tested in N<sub>2</sub> gas, which offers us larger signal and hence better calibration sensitivity relative to a He medium. We also tested a couple muon chambers in He to confirm that the choice of gas introduces no bias in the relative calibration.

The muon monitor calibrations are somewhat more complicated because of the large number of muon monitor chambers in comparison to the hadron monitor, and because of the long duration of construction and calibration of the muon monitors which led to potential temporal systematics such as electronics drifts or pressure and temperature changes. As discussed in Section 3.3, correction factors were derived for gas pressure and temperature variation which should maintain a relative calibration of individual chambers within the array to within 1%. Table 2 summarizes our expectation for all the systematic uncertainties in the relative calibration factors.

These correction procedures were demonstrated to work well on the reference chamber, which is more sensitive to such variations than are the muon chambers being calibrated. Figures 16 and 17 showed that the reference chamber signal, which could vary by 20% over the course of the 400 days of muon chamber testing, could be brought to 0.6% consistency, in agreement with the expectation in Table 2.

It was impractical to repeat the muon chamber calibrations for multiple iterations, as was done for the hadron monitor. However, we did test tube 26 at five different conditions spread out in time over the duration of the 400 days. The data is tabulated in Table 3. Listed are the pressures and temperatures of each test, in addition to the measured currents of the chamber being irradiated by the 1 Ci source, currents from each chamber when it is not being irradiated by the 1 Ci source (ie: is exposed only to its internal 1  $\mu$ Ci Am<sup>241</sup> source), and reference chamber currents. Pressures varied over 20 torr, and temperatures ranged from 72°F to 78°F. The bottom two rows of each table offer a measure of the percent correspondence between different chambers and different tests before and after pressure and temperature corrections. Two conclusions are drawn: 1) the multiple tests provide a 1% agreement for any given chamber, and 2) the chambers all scale the same way with pressure and temperature, so that the relative calibration maintains its integrity. The spread in the

plateau current values for a given chamber include variations due to source placement and readout, so the 1% agreement is inclusive of all of our sources of error.

Tables 5-8 show the irradiated plateau measurement and the non-irradiated plateau measurement for all muon chambers. The irradiated current of Tube 26, chamber 1, is scaled to one, and scale factors are derived for all chambers by the same normalization. The chambers are labeled by alcove and channel number, with channels corresponding to the mapping of Figure 3. Also given are the corresponding tube and chamber numbers.

## 6 Acknowledgements

Special thanks to Tracy Tipping of the Office of Environmental Health and Safety at the University of Texas, Marta Lang who assisted with conducting the calibration scans, and Jack Clifford of the UT Dept. of Physics Machine Shop for valuable assistance on this project.

## References

- [1] "The Hadron Monitor," NuMI-B-846 (July 2002).
- [2] "The Muon Monitor," NuMI-B-847 (July 2002).
- [3] D. Harris, "Specifications for the Downstream Hadron Monitor," NuMI-B-785 (Nov., 2001)
- [4] D. Harris, "Specifications for the Muon Monitors," NuMI-B-756 (June, 2001).
- [5] Y. Wang, CRC Handbook of Radioactive Nuclides (Cleveland: Chemical Rubber Co), 1969.
- [6] Keithley Instruments, Inc., Cleveland, OH.
- [7] Mindtel, Inc.
- [8] Applied Data Sciences, Inc., Dallas, TX.
- [9] MKS Instruments, Inc., Wilmington, MS.

	Pressure	Temp	Gas	Irradiated	Non-irrad	Ref. Ch.	Irrad corr to "Nominal"	Ref corr to "Nominal"	Raw Calib to Ch#1	Final Calib to Ch#1
Chamber 1	789.7	78	N2	125.5	6.45	105.05	126.09	100.56	1.000	1.000
	811.4	78	N2	128	6.45	93.7	126.58	99.13	1.000	1.000
	790.5	72	N2	126.6	7	100.6	126.55	100.83	1.000	1.000
	778.5	74	N2	124.5	6.45	106.5	125.76	99.79	1.000	1.000
	792.1	78	He	27.275	2.15	82.1	27.28	82.10	1.000	1.000
Chamber 2	788.1	78	N2	123	6	104.9	123.74	99.68	0.980	0.981
	811.7	78	N2	125.85	5.6	94.45	124.40	100.02	0.983	0.983
	788.2	72	N2	*	*	100.4	*	99.58	*	*
	778.5	74	N2	122.25	5.65	106.4	123.51	99.69	0.982	0.982
	791	77	He	26.85	2	82.05	26.85	82.05	0.984	0.984
Chamber 3	787	78	N2	124.5	6	104.7	125.34	98.98	0.992	0.994
	811.7	78	N2	127.5	6	94.45	126.05	100.02	0.996	0.996
	790	72	N2	126.25	6.5	100.25	126.25	100.25	0.997	0.998
	778.2	74	N2	124.1	6.2	106.3	125.38	99.46	0.997	0.997
	790.2	78	He	27.55	2.15	82.05	27.55	82.05	1.010	1.010
Chamber 4	786	78	N2	124.75	6.1	104.6	125.69	98.42	0.994	0.997
	811.4	78	N2	127.5	6.15	94	126.08	99.43	0.996	0.996
	790	72	N2	125.7	6.65	100.4	125.70	100.40	0.993	0.993
	779	74	N2	125.2	6.45	106.1	126.41	99.62	1.006	1.005
	790.2	78	He	27.35	1.85	82.05	27.35	82.05	1.003	1.003
Chamber 5	784.2	78	N2	128.25	7.3	104.35	129.35	97.35	1.022	1.026
	811.4	78	N2	131.25	7.25	93.9	129.83	99.33	1.025	1.026
	789.8	72	N2	129.7	8.1	100.45	129.72	100.36	1.024	1.025
	779.2	74	N2	128.3	7.3	106	129.49	99.61	1.031	1.030
	789	78	He	28.6	2.5	82.05	28.60	82.05	1.049	1.049
Chamber 6	791.6	78	N2	123.5	6.4	103.2	123.92	99.58	0.984	0.983
	811.4	78	N2	124.5	6.35	93.9	123.08	99.33	0.973	0.972
	789.3	72	N2	124.95	6.45	100.4	125.02	100.08	0.987	0.988
	779.3	74	N2	123.1	6.55	105.85	124.28	99.51	0.989	0.988
	788.7	78	He	27.55	2.4	82.1	27.55	82.10	1.010	1.010
Chamber 7	791.5	78	N2	123.25	2.6	103.2	123.67	99.54	0.982	0.981
	811.7	78	N2	124.5	2.6	93.75	123.05	99.32	0.973	0.972
	789.1	72	N2	124.75	3.25	100.4	124.83	99.99	0.985	0.986
	779.2	74	N2	121.75	2.75	105.8	122.94	99.41	0.978	0.978
	788.6	78	He	26.55	0.85	82.1	26.55	82.10	0.973	0.973
Chamber 8	790.6	78	N2	127.75	6.95	103.1	128.26	99.02	1.018	1.017
	811.4	78	N2	129.75	7	93.55	128.33	98.98	1.014	1.014
	789.8	72	N2	129.75	7.5	100.35	129.77	100.26	1.025	1.025
	779.2	74	N2	126.95	7.2	105.9	128.14	99.51	1.020	1.019
	788.5	78	He	28.3	0.9	82.15	28.30	82.15	1.038	1.038
Chamber 9	790.2	78	N2	122.75	4.1	103.1	123.30	98.84	0.978	0.978
	811.7	78	N2	124.8	4.2	93.45	123.35	99.02	0.975	0.974
	788.6	72	N2	125	4.9	100.3	125.13	99.66	0.987	0.989
	779.2	74	N2	121.35	4.3	105.9	122.54	99.51	0.975	0.974
	788.5	78	He	26.6	1.3	82.1	26.60	82.10	0.975	0.975

Table 3: Five sets of calibration data for all chambers of muon tube 26.

\* Chamber did not read out for this test

Chamber	HeCal1 air/He mix >285ppm	HeCal2 215-170 ppm	HeCal2 Corrected	HeCal3 170 ppm	HeCal4 90-90.5 ppm	HeCal5 90-90.5 ppm	Scale Factors
1	0.88	0.93	0.92		0.89	0.89	1.13
2	0.93	0.97	0.96		0.95	0.94	1.05
3	0.88	0.90	0.90		0.89	0.89	1.13
4	1.03	1.03	1.03		1.02	1.02	0.98
5	0.92	0.94	0.94		0.94	0.94	1.06
6	0.88	0.89	0.89		0.90	0.91	1.11
7	0.95	0.96	0.95		0.96	0.97	1.04
8	1.02	1.01	1.01		0.99	1.00	1.01
9	0.97	1.07	1.07		1.05	1.06	0.95
10	0.97	0.99	0.99		0.99	0.99	1.01
11	0.95	0.96	0.96		0.96	0.96	1.04
12	0.94	0.95	0.95		0.96	0.96	1.04
13	0.85	0.85	0.85		0.86	0.86	1.17
14	0.98	0.98	0.98		0.99	1.00	1.01
15	0.96	0.98	0.98		0.99		1.01
16	0.89	0.91	0.91		0.91		1.10
17	0.84	0.86	0.86		0.86		1.16
18	0.93	0.93	0.93		0.93		1.07
19	1.04	1.00	1.00		1.05		0.96
20	0.90	0.89	0.89		0.86		1.16
21	0.90	0.91	0.91		0.93		1.07
22	0.95	0.96	0.96		0.96		1.04
23	0.92	0.92	0.92		0.92		1.08
24	0.94	0.94	0.94		0.94		1.07
25	1.00	1.00	1.00		1.00		1.00
26	0.94	0.93	0.93		0.93		1.08
27	0.91	0.91	0.91		0.91		1.09
28	0.98	0.99	0.99		0.99		1.01
29	0.91	0.91	0.91		0.92		1.08
30	0.93	0.93	0.93		0.94		1.06
31	1.03	1.03	1.03		1.03		0.97
32	0.98	0.98	0.98		0.98		1.02
33	0.95	0.98	0.98		0.97		1.03
34	0.93	0.95	0.95		0.96		1.04
35	0.91	0.91	0.91		0.91		1.09
36	0.98	0.97	0.97		0.98		1.02
37	0.96	0.95	0.95		0.97		1.04
38	0.93	0.91	0.91		0.94		1.07
39	0.93	0.94	0.94		0.95		1.05
40	1.01	1.00	1.00		1.02		0.98
41	1.07	1.07	1.07		1.08		0.92
42	0.93	0.98	0.98		0.94		1.07
43	1.06	1.04	1.04	1.06	1.07		0.94
44	0.95	0.94	0.94	0.94	0.95		1.06
45	0.92	0.90	0.90	0.92	0.93		1.08
46	1.03	1.02	1.02	1.02	1.02		0.98
47	0.91	0.91	0.91	0.92	0.93		1.07
48	0.84	0.85	0.85	0.85	0.86		1.16
49	0.96	0.96	0.96	0.97	0.98		1.03

Table 4: Table of normalized plateau signals in the Hadron monitor ion chambers for 5 sets of measurements and the scale factors. We take the nominal calibration constants to be HeCal4.

Alcove 1											
Channel	Tube	Chamber	Irad			Channel	Tube	Chamber	Irad		
			Current (pA)	Non-Irad Current (pA)	Scale Factor				Current (pA)	Non-Irad Current (pA)	Scale Factor
1	31	9	123.72	6.24	1.017	41	24	5	124.85	7.18	1.004
2	31	8	123.26	5.99	1.021	42	24	4	123.94	6.19	1.012
3	31	7	124.60	6.55	1.010	43	24	3	124.33	6.32	1.008
4	31	6	122.56	6.20	1.027	44	24	2	122.89	5.89	1.020
5	31	5	121.49	6.42	1.036	45	24	1	124.36	6.29	1.009
6	31	4	122.45	6.20	1.028	46	13	9	123.63	4.08	1.016
7	31	3	123.60	5.87	1.018	47	13	8	124.61	6.77	1.009
8	31	2	123.04	5.81	1.045	48	13	7	128.60	7.50	0.978
9	31	1	122.84	6.05	1.026	49	13	6	124.80	6.99	1.007
10	6	9	123.39	3.76	1.024	50	13	5	123.88	6.35	1.015
11	6	8	127.79	6.43	0.989	51	13	4	124.20	6.90	1.012
12	6	7	128.62	7.20	0.982	52	13	3	123.39	6.26	1.019
13	6	6	126.18	5.74	1.002	53	13	2	124.73	6.20	1.008
14	6	5	126.89	6.34	0.997	54	13	1	123.70	6.23	1.016
15	6	4	125.46	6.42	1.009	55	20	9	128.48	5.68	0.976
16	6	3	126.50	5.88	1.000	56	20	8	127.94	6.38	0.980
17	6	2	129.20	6.81	0.980	57	20	7	126.90	6.00	0.989
18	6	1	126.42	6.76	1.001	58	20	6	125.86	7.38	0.997
19	16	9	126.39	5.14	0.995	59	20	5	126.96	6.20	0.988
20	16	8	127.73	7.40	0.985	60	20	4	127.45	7.24	0.985
21	16	7	126.02	7.26	0.999	61	20	3	125.49	6.21	1.000
22	16	6	122.49	6.55	1.028	62	20	2	127.42	6.34	0.984
23	16	5	126.30	6.76	0.996	63	20	1	125.09	6.19	1.003
24	16	4	126.21	6.66	0.997	64	2	9	125.16	4.73	1.007
25	16	3	128.17	6.87	0.981	65	2	8	126.83	5.83	0.993
26	16	2	126.16	6.64	0.997	66	2	7	129.63	7.30	0.972
27	16	1	126.21	6.39	0.997	67	2	6	123.76	5.19	1.018
28	27	9	125.79	6.18	0.999	68	2	5	124.72	4.54	1.011
29	27	8	128.39	6.11	0.980	69	2	4	126.73	7.43	0.995
30	27	7	125.12	6.16	1.005	70	2	3	123.70	4.14	1.019
31	27	6	129.30	5.71	0.973	71	2	2	122.21	4.16	1.032
32	27	5	124.53	5.08	1.010	72	2	1	125.24	6.68	1.007
33	27	4	123.62	7.03	1.017	73	19	9	125.42	7.65	1.000
34	27	3	125.90	6.53	0.999	74	19	8	129.24	7.46	0.972
35	27	2	123.38	6.50	1.020	75	19	7	125.92	6.57	0.997
36	27	1	126.88	6.92	0.992	76	19	6	124.45	6.20	1.009
37	24	9	125.11	6.58	1.005	77	19	5	125.55	6.42	1.000
38	24	8	123.31	3.25	1.019	78	19	4	124.01	6.14	1.013
39	24	7	126.01	6.76	0.999	79	19	3	128.09	6.96	0.980
40	24	6	125.63	6.54	1.002	80	19	2	123.97	6.26	1.013
						81	19	1	120.59	5.96	1.042

Table 5: Scale factors for channels 1-81 in Alcove 1. Channel number refers to the indexing scheme used by the readout electronics. Also given are the tube and chamber numbers for calibration referencing.

Alcove 2											
Channel	Tube	Chamber	Irad			Channel	Tube	Chamber	Irad		
			Current (pA)	Non-Irad Current (pA)	Scale Factor				Current (pA)	Non-Irad Current (pA)	Scale Factor
1	18	9	124.96	5.61	1.001	41	10	5	129.05	6.77	0.972
2	18	8	130.54	6.88	0.959	42	10	4	126.88	5.57	0.988
3	18	7	126.78	6.14	0.987	43	10	3	129.38	6.24	0.969
4	18	6	122.14	4.90	1.024	44	10	2	128.35	6.81	0.977
5	18	5	123.92	5.51	1.009	45	10	1	125.12	6.80	1.002
6	18	4	124.96	5.92	1.001	46	32	9	126.43	6.39	1.001
7	18	3	125.30	6.52	0.998	47	32	8	128.55	5.73	0.984
8	18	2	125.51	7.08	0.997	48	32	7	127.76	6.39	0.990
9	18	1	124.56	6.34	1.004	49	32	6	124.16	6.10	1.019
10	8	9	120.98	3.52	1.038	50	32	5	125.43	6.11	1.005
11	8	8	129.00	7.89	0.974	51	32	4	127.26	6.57	0.990
12	8	7	125.55	7.61	1.001	52	32	3	124.26	5.82	1.014
13	8	6	126.29	6.08	0.995	53	32	2	123.70	5.75	1.018
14	8	5	122.59	5.61	1.026	54	32	1	120.77	5.98	1.043
15	8	4	125.22	6.20	1.004	55	21	9	122.25	5.62	1.005
16	8	3	126.80	7.78	0.991	56	21	8	122.38	7.68	0.986
17	8	2	123.54	5.68	1.017	57	21	7	120.16	6.97	1.028
18	8	1	124.01	7.23	1.014	58	21	6	123.98	6.95	1.012
19	9	9	125.22	5.93	1.007	59	21	5	121.28	7.05	1.033
20	9	8	124.70	6.41	1.011	60	21	4	123.75	7.09	1.010
21	9	7	127.29	6.82	0.991	61	21	3	121.89	5.26	1.042
22	9	6	126.31	7.95	0.999	62	21	2	127.02	6.23	1.024
23	9	5	121.39	5.58	1.040	63	21	1	124.63	6.98	1.025
24	9	4	120.53	4.95	1.048	64	11	9	124.67	6.04	0.956
25	9	3	124.40	5.91	1.015	65	11	8	127.34	6.87	0.976
26	9	2	123.64	7.86	1.022	66	11	7	125.15	5.84	1.014
27	9	1	126.05	5.68	1.003	67	11	6	126.04	6.33	1.003
28	14	1	125.82	4.51	1.004	68	11	5	124.54	6.39	1.000
29	14	2	127.46	7.30	0.991	69	11	4	124.63	6.79	0.988
30	14	3	126.83	5.44	0.996	70	11	3	123.27	5.02	0.995
31	14	4	121.22	5.88	1.043	71	11	2	128.20	6.51	0.978
32	14	5	125.02	6.08	1.013	72	11	1	130.85	6.90	1.000
33	14	6	125.82	6.90	1.006	73	23	9	121.82	6.06	1.011
34	14	7	125.77	6.43	1.006	74	23	8	125.07	6.33	1.030
35	14	8	123.33	5.74	1.027	75	23	7	123.33	6.41	1.002
36	14	9	123.08	5.95	1.029	76	23	6	127.22	8.18	0.986
37	10	9	124.68	4.21	1.010	77	23	5	123.92	4.60	1.008
38	10	8	128.92	7.08	0.977	78	23	4	127.05	6.05	0.982
39	10	7	125.63	7.17	1.002	79	23	3	125.07	5.80	1.013
40	10	6	122.02	6.15	1.032	80	23	2	121.61	6.21	0.999
						81	23	1	123.89	6.29	1.026

Table 6: Scale factors for channels 1-81 in Alcove 2. Channel number refers to the indexing scheme used by the readout electronics. Also given are the tube and chamber numbers for calibration referencing.

Alcove 3											
Channel	Tube	Chamber	Irad			Channel	Tube	Chamber	Irad		
			Current (pA)	Non-Irad Current (pA)	Scale Factor				Current (pA)	Non-Irad Current (pA)	Scale Factor
1	15	9	128.53	7.02	0.982	41	1	5	124.35	3.92	1.010
2	15	8	125.63	5.02	1.006	42	1	4	126.68	6.82	0.992
3	15	7	128.68	6.20	0.981	43	1	3	126.31	6.99	0.995
4	15	6	122.88	5.53	1.029	44	1	2	125.26	6.55	1.003
5	15	5	123.88	7.06	1.021	45	1	1	120.96	4.01	1.038
6	15	4	123.48	6.68	1.024	46	29	9	121.48	3.49	1.037
7	15	3	122.04	5.65	1.037	47	29	8	127.32	6.58	0.990
8	15	2	124.50	6.58	1.017	48	29	7	122.36	4.76	1.031
9	15	1	123.38	6.07	1.027	49	29	6	122.93	5.24	1.027
10	4	9	130.48	6.97	0.973	50	29	5	124.61	6.81	1.013
11	4	8	126.64	3.31	1.002	51	29	4	121.03	5.23	1.046
12	4	7	128.51	7.51	0.988	52	29	3	124.28	6.68	1.017
13	4	6	130.54	6.48	0.972	53	29	2	122.00	6.09	1.036
14	4	5	127.78	4.40	0.997	54	29	1	127.73	6.95	0.989
15	4	4	126.32	4.26	1.009	55	5	9	124.28	4.36	1.018
16	4	3	126.85	6.76	1.004	56	5	8	128.99	6.36	0.980
17	4	2	129.61	7.03	0.982	57	5	7	126.23	6.65	1.002
18	4	1	126.88	6.61	1.003	58	5	6	125.23	5.63	1.010
19	26	9	122.73	4.12	1.022	59	5	5	122.87	5.36	1.031
20	26	8	127.65	6.93	0.983	60	5	4	125.16	6.20	1.011
21	26	7	123.29	2.61	1.019	61	5	3	124.15	4.74	1.019
22	26	6	123.45	6.43	1.018	62	5	2	124.70	5.80	1.015
23	26	5	128.22	7.30	0.975	63	5	1	127.19	5.49	0.995
24	26	4	124.69	6.18	1.003	64	30	9	123.62	5.91	1.018
25	26	3	124.49	6.02	1.006	65	30	8	123.35	5.06	1.021
26	26	2	122.97	5.65	1.019	66	30	7	123.11	6.14	1.022
27	26	1	125.44	6.44	1.000	67	30	6	125.87	7.65	1.000
28	25	9	124.92	6.76	1.010	68	30	5	127.85	6.51	0.984
29	25	8	126.36	6.36	0.998	69	30	4	125.22	5.95	1.005
30	25	7	124.55	6.50	1.012	70	30	3	123.15	6.49	1.025
31	25	6	124.43	6.77	1.013	71	30	2	123.89	6.78	1.037
32	25	5	122.53	4.46	1.029	72	30	1	121.45	5.27	1.037
33	25	4	122.48	6.47	1.029	73	28	9	125.91	7.26	0.996
34	25	3	124.16	6.78	1.015	74	28	8	122.96	4.60	1.020
35	25	2	124.77	7.58	1.010	75	28	7	124.90	6.62	1.004
36	25	1	124.83	6.38	1.009	76	28	6	131.48	6.69	0.953
37	1	9	124.08	4.97	1.017	77	28	5	125.69	6.74	0.998
38	1	8	128.11	5.97	0.985	78	28	4	127.44	7.46	0.984
39	1	7	123.10	3.29	1.026	79	28	3	126.68	6.44	0.991
40	1	6	126.83	7.36	0.995	80	28	2	123.06	6.51	1.020
						81	28	1	126.06	5.64	0.996

Table 7: Scale factors for channels 1-81 in Alcove 3. Channel number refers to the indexing scheme used by the readout electronics. Also given are the tube and chamber numbers for calibration referencing.

Spare Tubes									
Irrad					Irrad				
Tube	Chamber	Current (pA)	Non-Irrad Current (pA)	Scale Factor	Tube	Chamber	Current (pA)	Non-Irrad Current (pA)	Scale Factor
3	1	125.03	6.88	0.984	12	1	124.55	6.14	0.987
3	2	125.66	5.92	0.994	12	2	122.83	4.94	0.993
3	3	126.74	7.42	1.022	12	3	121.54	6.31	0.995
3	4	125.10	5.73	0.992	12	4	123.23	7.30	1.006
3	5	126.26	6.57	1.000	12	5	124.49	5.92	1.003
3	6	127.55	6.94	1.009	12	6	124.37	6.37	1.013
3	7	123.86	4.50	0.996	12	7	125.81	6.25	1.028
3	8	127.43	4.71	1.005	12	8	126.05	4.91	1.016
3	9	128.67	6.53	1.010	12	9	126.79	7.11	1.003
7	1	124.39	7.11	0.997	17	1	120.24	5.64	0.997
7	2	126.41	7.32	1.000	17	2	123.96	7.67	0.955
7	3	125.20	6.83	0.989	17	3	126.02	7.50	0.993
7	4	124.99	6.64	0.993	17	4	125.15	6.02	0.970
7	5	126.14	7.03	0.993	17	5	128.40	6.88	0.978
7	6	126.08	6.75	1.002	17	6	129.40	8.38	1.003
7	7	126.72	6.53	1.000	17	7	126.51	8.33	0.996
7	8	125.34	6.09	0.990	17	8	125.29	6.12	1.013
7	9	125.70	6.04	1.006	17	9	126.76	7.68	1.045

Table 8: Scale factors for the spare tubes. Given are the tube and chamber numbers for calibration referencing.

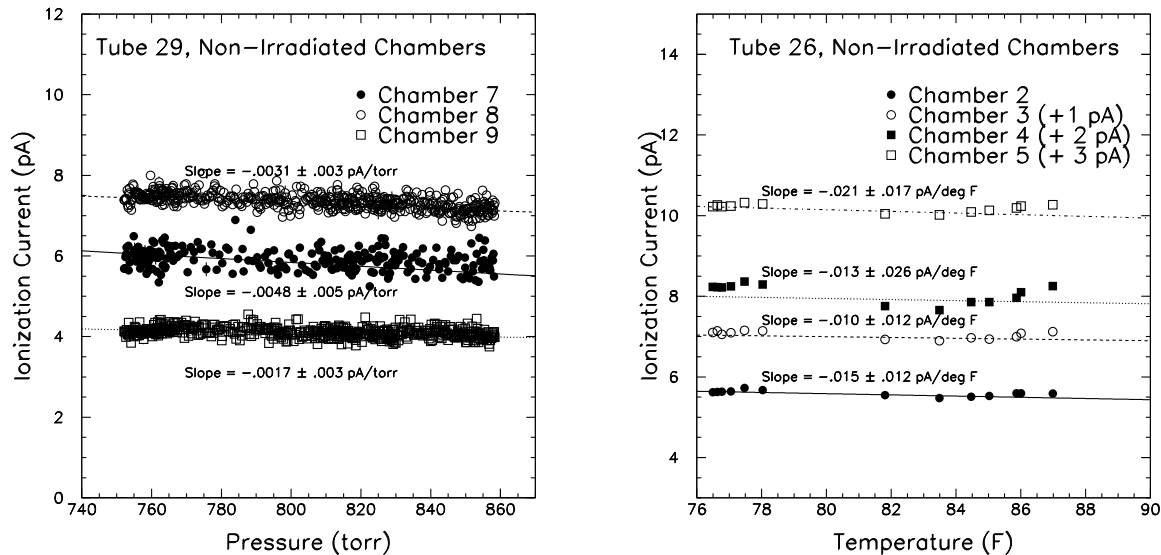


Figure 24: Variation of the ionization current in a muon chamber arising from its internal  $1 \mu\text{Ci Am}^{241}$  source as measured in  $\text{N}_2$  gas: (left) variation with pressure. (right) variation with temperature.

## A Study of Muon Tube Internal Sources

Initially it was envisaged to use the small  $1 \mu\text{Ci Am}^{241}$  alpha sources mounted on each ion chamber in the muon tubes to perform day-to-day calibrations. As described in this note, however, a simpler procedure was developed which required only a single calibration factor for temperature and a single calibration factor for pressure, as well as instrumentation which reliably read out pressure and temperature. This obviated the need for the more complicated procedure of deriving 243 calibration slopes of the alpha sources *vs.* temperature and pressure.

We furthermore found that the alpha sources pose an additional complication not anticipated when the muon tubes were designed: the alpha's must enter the parallel plate ion chambers from one side of the rectangular plates, and must pass through approximately 1.5-2.0 cm of gas before entering the sensitive volume of the ion chamber. Thus, while naively one expects ionization yield to increase with increased gas density (larger pressure or lower temperature), we observed more complicated, and not consistent behaviour from chamber to chamber. In some chambers, increased gas density actually caused the ionization current to drop. Our conjecture was that the increased gas density caused some of the alpha particles to range out in the gas prior to entering the ion chamber's sensitive volume. This effect, competing with the larger ionization yield anticipated, caused inconsistent behaviour amongst chambers.

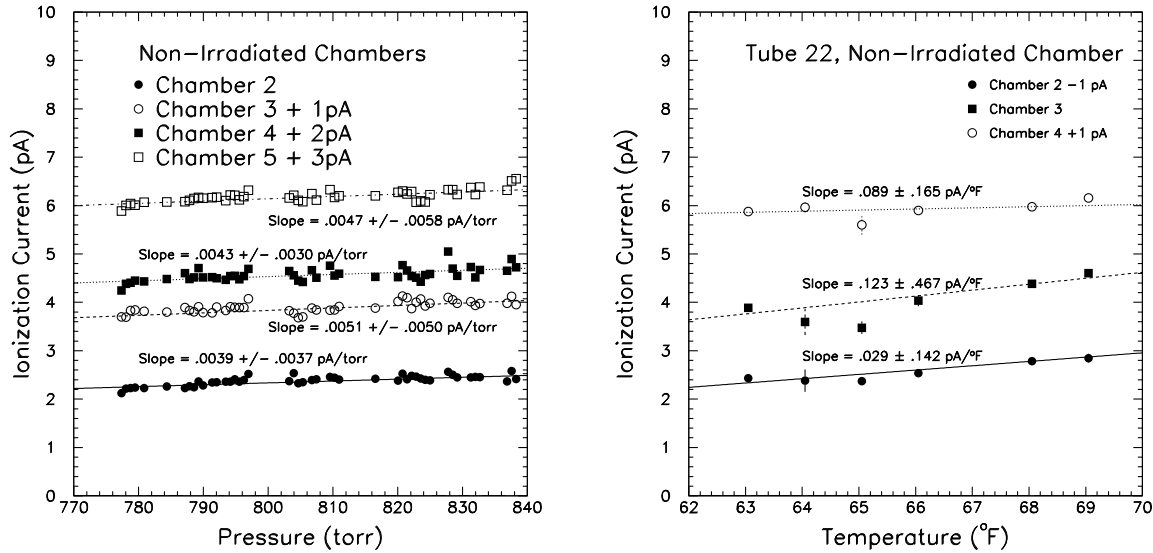


Figure 25: Variation of the ionization current in a muon chamber arising from its internal  $1 \mu\text{Ci Am}^{241}$  source as measured in He gas: (left) variation with pressure. (right) variation with temperature.

We also found that the sensitivity of the small alpha sources to pressure and temperature changes was quite poor, owing to the small signal size and relatively indirect measurement technique. Furthermore, because the alpha sources actually experience the opposite trend with pressure and temperature as would beam particles, calibration via this technique appeared implausible.

The data from the small alpha sources are shown in Figures 24 and 25.